

Supplemental Information

Effect of Polymer Chemistry on the Linear Viscoelasticity of Complex Coacervates

Yalin Liu,¹ Cristiam F. Santa Chalarca,² R. Nicholas Carmean,³ Rebecca A. Olson,³ Jason Madinya,⁴
Brent S. Sumerlin,³ Charles E. Sing,⁴ Todd Emrick,² Sarah L. Perry^{1*}

¹ Department of Chemical Engineering, University of Massachusetts Amherst, Amherst, MA 01003, USA

² Department of Polymer Science & Engineering, University of Massachusetts Amherst, Amherst, MA 01003, USA

³ George & Josephine Butler Polymer Research Laboratory, Center for Macromolecular Science & Engineering, Department of Chemistry, University of Florida, Gainesville, FL 32611, USA

⁴ Department of Chemical and Biomolecular Engineering, University of Illinois at Urbana-Champaign, Urbana, IL 61801, USA

*Author to whom correspondence should be addressed. Electronic mail: perrys@engin.umass.edu

Monomer Synthesis

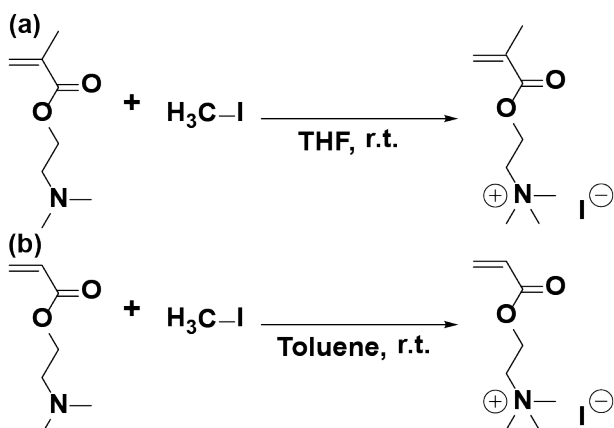


Figure S1. (a) The [2-(methacryloyloxy)ethyl]trimethylammonium iodide monomer was synthesized by alkylation of 2-(dimethylamino)ethyl methacrylate with iodomethane in tetrahydrofuran (THF, ACS grade). (b) [2-(acryloyloxy)ethyl]trimethylammonium iodide monomer was synthesized by alkylation of 2-(dimethylamino)ethyl methacrylate with iodomethane in toluene.

Monomer Characterization

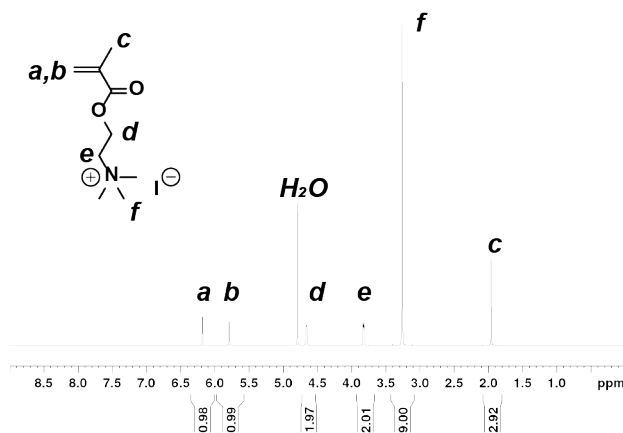


Figure S2. ¹H NMR spectrum for the synthesized monomer [2-(methacryloyloxy)ethyl]trimethylammonium iodide.

Polymer Characterization

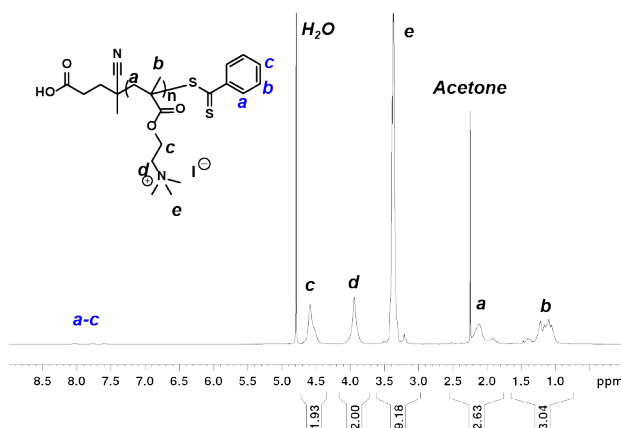


Figure S3. ¹H NMR spectrum for the synthesized polycation poly([2-(methacryloyloxy)ethyl]trimethylammonium) (PTMAEMA) with length N = 50.

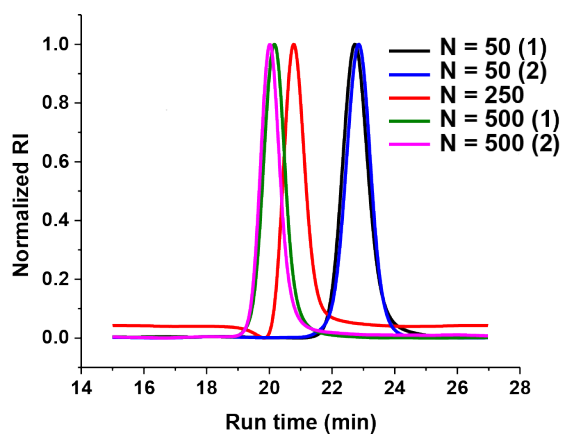


Figure S4. Gel permeation chromatography traces showing the normalized refractive index signal as a function of run time for the synthesized polycation poly([2-(methacryloyloxy)ethyl]trimethylammonium) (PTMAEMA) with degree of polymerization N = 50, 250, and 500.

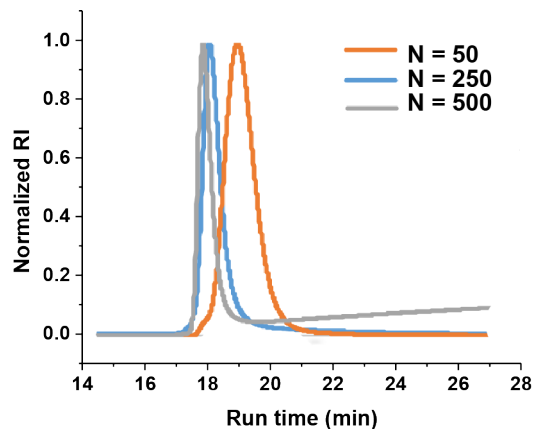


Figure S5. Gel permeation chromatography traces showing the normalized refractive index signal as a function of run time for the synthesized polyanion poly(3-sulfopropyl methacryloyl) (PSPMA) with degree of polymerization $N = 50$, 250, and 500.

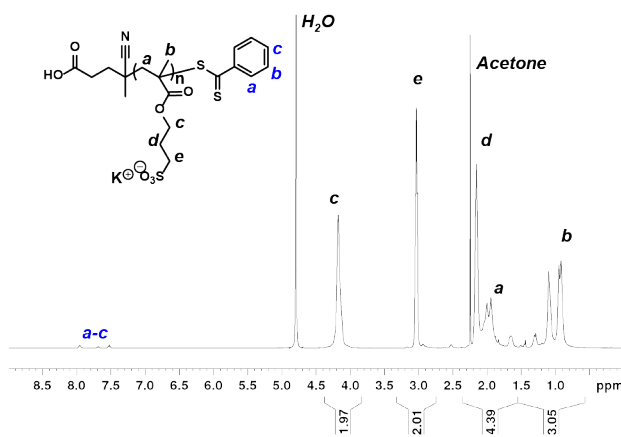


Figure S6. ^1H NMR spectrum for the synthesized polyanion poly(3-sulfopropyl methacryloyl) (PSPMA) with length $N = 50$.

Table S1. Table of properties for PSPMA.

Sample PSPMA	Feed [M]: [CTA]:[I]	[M] ₀ (wt%)	Polymerization time (h)	N	Conv ^a (%)	M _n ^b (kDa)	Đ ^b
DP 50	50:1:0.2	19.657	16	45	>99	16.7	1.05
DP 250	250:1:0.2	19.742	16	230	>99	56.2	1.10
DP 500	500:1:0.2	19.752	48	450	>99	116.8	1.28

^aEstimated from the ¹H NMR analysis of the crude polymerization product in D₂O.

^bM_n and Đ calculated from GPC traces measured using 80/20 v/v mixture of aqueous 0.1 M sodium nitrate (NaNO₃, Sigma Aldrich) and acetonitrile (C₂H₃N, ACS Grade, Fisher) as the eluent.

Table S2. Table of properties for PTMAEMA.

Sample PTMAEMA	Feed [M]: [CTA]:[I]	[M] ₀ (wt%)	Polymerization time (h)	N	Conv ^a (%)	M _n ^b (kDa)	Đ ^b
DP 50(1)	50:1:0.2	22.913	16	49	98.6	28.2	1.04
DP 50(2)	50:1:0.2	22.913	16	47	N.M	27.7	1.04
DP 250	250:1:0.2	23.007	16	237	94.7	84.9	1.05
DP 500(1)	500:1:0.2	23.019	48	460	91.9	129.4	1.11
DP 500(2)	500:1:0.2	23.019	48	476	95.1	135.5	1.09

^aEstimated from the ¹H NMR analysis of the crude polymerization product in D₂O.

^bM_n and Đ calculated from GPC traces measured using trifluoroethanol (TFE) as the eluent and poly(methyl methacrylate) (PMMA) standards.

Table S3. Table of properties for PAMPS.

Sample PAMPS	N	M_n^a (kDa)	\bar{D}^a
DP 250	388	69.8	2.27
DP 1000	1206	206.1	1.23
DP 2000	1582	283.5	1.10

^a M_n and \bar{D} calculated from GPC traces measured using 80/20 v/v mixture of aqueous 0.1 M sodium nitrate (NaNO₃, Sigma Aldrich) and acetonitrile (C₂H₃N, ACS Grade, Fisher) as the eluent.

Table S4. Table of properties for PTMAEA.

Sample PTMAEA	N	M_n^a (kDa)	\bar{D}^a
DP 250	255	40.6	1.21
DP 1000	1053	166.7	1.22
DP 2000	2450	388.4	1.24

^a M_n and \bar{D} calculated from GPC traces measured using trifluoroethanol (TFE) as the eluent and poly(methyl methacrylate) (PMMA) standards.

Phase Diagram Characterization

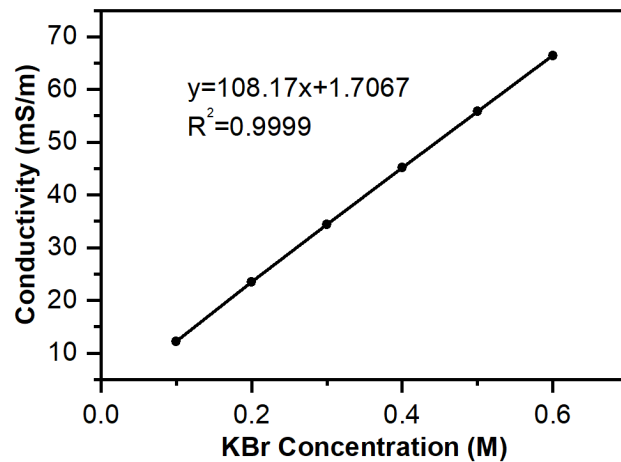


Figure S7. Calibration curve for the solution conductivity as a function of KBr concentration.

Propagation of Error Calculations:

Error bars associated with binodal curve data are the result of uncertainty associated with the measurement of the coacervate volume and the conductivity of the supernatant. Furthermore, these errors coupled with uncertainty associated with the linear fit to the data shown in **Figure S7** when propagated through our calculations.

The concentration of salt in the supernatant ($C_{salt-sup}$) was determined via conductivity measurements (S_{sup}) and the use of a calibration curve (slope of m , intercept of b).

$$C_{salt-sup} = \frac{S_{sup}-b}{m} \quad (S1)$$

The error in the conductivity measurements (δS_{sup}) was ± 0.1 mS/cm. The uncertainty associated with the calibration curve (δm , δb) was determined using the LINEST function in Excel.

$$\delta C_{salt-sup} = \sqrt{\frac{1}{m^2} \delta S_{sup}^2 + \frac{1}{m^2} \delta b^2 + \left(\frac{S_{sup}-b}{m^2}\right)^2 \delta m^2} \quad (S2)$$

The concentration of salt in the coacervate ($C_{salt-coac}$) was determined using the law of mass action, knowing the concentration of salt in the supernatant ($C_{salt-sup}$), the volume of the supernatant (V_{sup}), the total concentration of salt added ($C_{salt-total}$), the total sample volume (V_{total}), and the volume of the coacervate (V_{coac}).

$$C_{salt-coac} = \frac{C_{salt-total}V_{total}-C_{salt-sup}V_{sup}}{V_{coac}} \quad (S3)$$

The uncertainty in the volumes of the supernatant and coacervate (δV_{sup} and δV_{coac}) was ± 0.1 mL. We assumed that the uncertainty of the total volume and the total salt concentration were negligible.

$$\delta C_{salt-coac} = \sqrt{\left(\frac{V_{sup}}{V_{coac}} \delta C_{salt-sup}\right)^2 + \left(\frac{C_{salt-sup}}{V_{coac}} \delta V_{sup}\right)^2 + \left(\frac{C_{salt-sup}V_{sup}-C_{salt-total}V_{total}}{V_{coac}^2} \delta V_{coac}\right)^2} \quad (S4)$$

The concentration of polymer in the coacervate ($C_{poly-coac}$) was determined again using the law of mass action, and assuming that the concentration of polymer in the supernatant was negligible.

$$C_{poly-coac} = \frac{C_{poly-total}V_{total}}{V_{coac}} \quad (S5)$$

$$\delta C_{poly-coac} = \frac{C_{poly-total}V_{total}}{V_{coac}^2} \delta V_{coac} \quad (S6)$$

Table S5. Summary of samples. All samples were prepared at a total polymer concentration of 0.045 M on a monomer basis. Error is associated with the uncertainty in coacervate volume measurements, uncertainty in supernatant conductivity measurements, linear fit to conductivity calibration data, and the associated propagation of error.

	As Prepared	Supernatant		Coacervate	
	C_{Salt} (M)	C_{Salt} (M)	C_{Polymer} (M)	C_{Salt} (M)	C_{Polymer} (M)
M50-50	0.1	0.124 ± 0.0024	0.0	0.044 ± 0.131	2.49 ± 0.28
	0.2	0.225 ± 0.0026	0.0	0.082 ± 0.129	2.24 ± 0.22
	0.3	0.327 ± 0.0029	0.0	0.137 ± 0.120	1.87 ± 0.16
	0.4	0.427 ± 0.0032	0.0	0.270 ± 0.117	1.60 ± 0.11
M250-250	0.2	0.225 ± 0.0026	0.0	0.067 ± 0.143	2.49 ± 0.28
	0.3	0.327 ± 0.0029	0.0	0.120 ± 0.131	2.04 ± 0.19
	0.4	0.428 ± 0.0032	0.0	0.206 ± 0.136	1.87 ± 0.16
	0.6	0.630 ± 0.0041	0.0	0.353 ± 0.150	1.60 ± 0.11
M500-500	0.3	0.326 ± 0.0029	0.0	0.125 ± 0.161	2.49 ± 0.28
	0.4	0.428 ± 0.0032	0.0	0.186 ± 0.149	2.04 ± 0.19
	0.5	0.528 ± 0.0036	0.0	0.329 ± 0.143	1.72 ± 0.13
	0.6	0.628 ± 0.0041	0.0	0.417 ± 0.150	1.60 ± 0.11
M50-500	0.1	0.124 ± 0.0024	0.0	0.028 ± 0.131	2.49 ± 0.28
	0.2	0.225 ± 0.0026	0.0	0.082 ± 0.129	2.24 ± 0.22
	0.3	0.327 ± 0.0029	0.0	0.137 ± 0.120	1.87 ± 0.16
	0.4	0.427 ± 0.0032	0.0	0.270 ± 0.117	1.60 ± 0.13
M500-50	0.1	0.124 ± 0.0024	0.0	0.028 ± 0.131	2.49 ± 0.28
	0.2	0.225 ± 0.0026	0.0	0.082 ± 0.129	2.24 ± 0.22
	0.3	0.327 ± 0.0029	0.0	0.137 ± 0.120	1.87 ± 0.16
	0.4	0.427 ± 0.0032	0.0	0.258 ± 0.126	1.72 ± 0.13
A250-250	0.05	0.073 ± 0.0024	0.0	0.060 ± 0.088	1.72 ± 0.13
	0.10	0.124 ± 0.0024	0.0	0.082 ± 0.084	1.60 ± 0.11
	0.15	0.173 ± 0.0025	0.0	0.140 ± 0.076	1.40 ± 0.09
	0.20	0.224 ± 0.0026	0.0	0.167 ± 0.075	1.32 ± 0.08
A1000-1000	0.45	0.459 ± 0.0034	0.0	0.202 ± 0.109	1.40 ± 0.09
	0.50	0.530 ± 0.0036	0.0	0.297 ± 0.109	1.32 ± 0.08
	0.55	0.579 ± 0.0039	0.0	0.397 ± 0.104	1.18 ± 0.06
A2000-2000	0.40	0.430 ± 0.0032	0.0	0.161 ± 0.109	1.49 ± 0.10
	0.45	0.458 ± 0.0034	0.0	0.230 ± 0.109	1.40 ± 0.09
	0.50	0.508 ± 0.0036	0.0	0.310 ± 0.103	1.24 ± 0.07
	0.55	0.579 ± 0.0039	0.0	0.406 ± 0.098	1.12 ± 0.06

Table S6. Binodal error analysis based on the assumption of no polymer vs. 5 mM of polymer (on a monomer basis) in the supernatant for the methacryloyl 50-50 system. The relative change in polymer concentration is approximately 11%, and is consistent across all samples.

Assume all polymer goes to the coacervate					Assume 5 mM monomer in the supernatant			
Total C_{salt} (M)	Coacervate		Supernatant		Coacervate		Supernatant	
	C_{salt} (M)	C_{poly} (M)	C_{salt} (M)	C_{poly} (M)	C_{salt} (M)	C_{poly} (M)	C_{salt} (M)	C_{poly} (M)
0.10	0.044	2.49	0.124	--	0.044	2.22	0.124	0.005
0.20	0.082	2.24	0.225	--	0.082	2.00	0.225	0.005
0.30	0.137	1.87	0.327	--	0.137	1.66	0.327	0.005
0.40	0.270	1.60	0.427	--	0.270	1.43	0.427	0.005

Table S7. Binodal error analysis based on the assumption of no polymer vs. 5 mM of polymer (on a monomer basis) in the supernatant for the acryloyl 250-250 system. The relative change in polymer concentration is approximately 11%, and is consistent across all samples.

Assume all polymer goes to the coacervate					Assume 5 mM monomer in the supernatant			
Total C_{salt} (M)	Coacervate		Supernatant		Coacervate		Supernatant	
	C_{salt} (M)	C_{poly} (M)	C_{salt} (M)	C_{poly} (M)	C_{salt} (M)	C_{poly} (M)	C_{salt} (M)	C_{poly} (M)
0.05	0.060	1.72	0.073	--	0.060	1.54	0.073	0.005
0.10	0.114	1.60	0.123	--	0.114	1.43	0.123	0.005
0.15	0.140	1.40	0.173	--	0.140	1.25	0.173	0.005
0.20	0.167	1.32	0.224	--	0.167	1.18	0.224	0.005

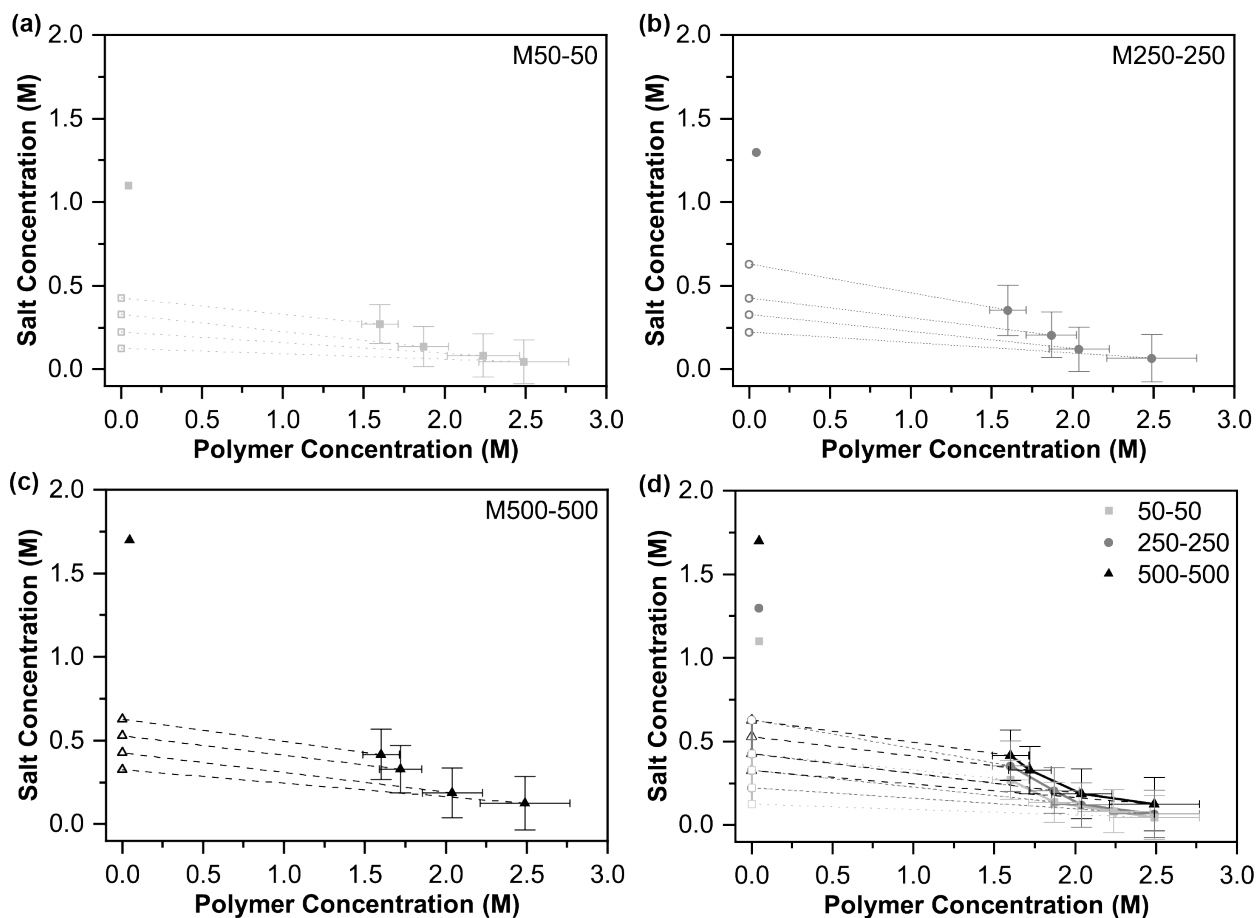


Figure S8. Experimentally determined salt-polymer phase diagrams for the complex coacervation of the methacryloyl polymers in the presence of KBr at a 1:1 stoichiometric charge ratio. We compare the data for length-matched polymers with a degree of polymerization $N_{\text{anion}}-N_{\text{cation}}$ of **(a)** 50-50, **(b)** 250-250, **(c)** 500-500, and **(d)** an overlay of all three data sets. The plots include data at low polymer concentration and high salt concentration obtained via turbidimetry and from direct measurements of the salt and polymer concentration present in the two phases. Tie lines connect data for corresponding coacervate (closed symbols) and supernatant (open symbols) samples. The unconnected symbols present at low polymer concentration and high salt concentration correspond to data obtained via turbidity analysis. Polymer concentration is on a monomer basis. Error bars in are based on the uncertainty of measurement and propagation of error.

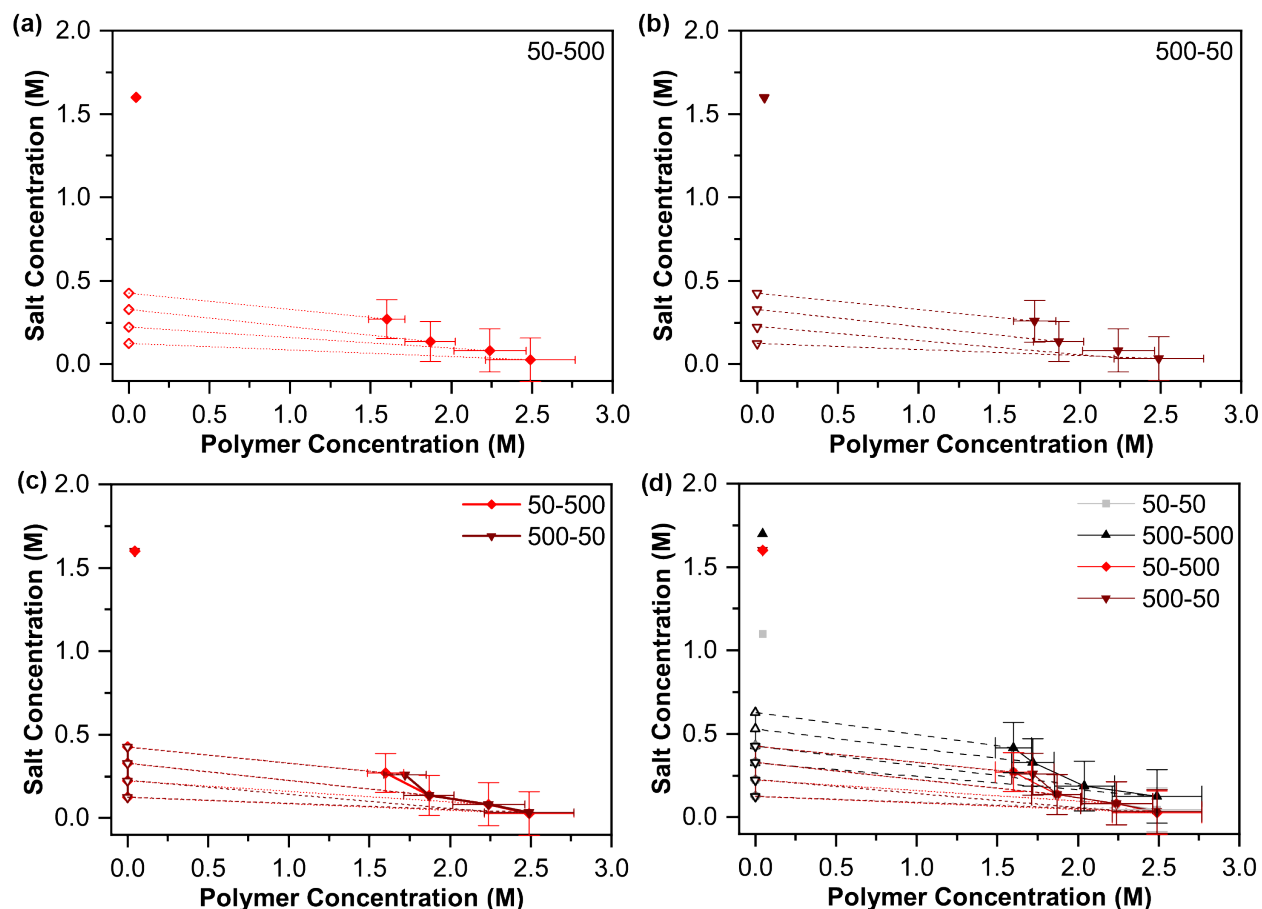


Figure S9. Experimentally determined salt-polymer phase diagrams for the complex coacervation of the methacryloyl polymers PSPMA and PTMAEMA in the presence of KBr at a 1:1 stoichiometric charge ratio. We compare the data for length-mismatched polymers with a degree of polymerization $N_{\text{anion}}-N_{\text{cation}}$ of (a) 50-500 and (b) 450-47. (c) An overlay of data for the two mismatched systems and (d) a comparison between the two mismatched systems (red) and the data for the short 50-50 (grey) and the long 500-50 (black) systems. Tie lines connect data for corresponding coacervate (closed symbols) and supernatant (open symbols) sample. The unconnected symbols present at low polymer concentration and high salt concentration correspond to data obtained via turbidity analysis. Error bars in are based on the uncertainty of measurement and propagation of error.

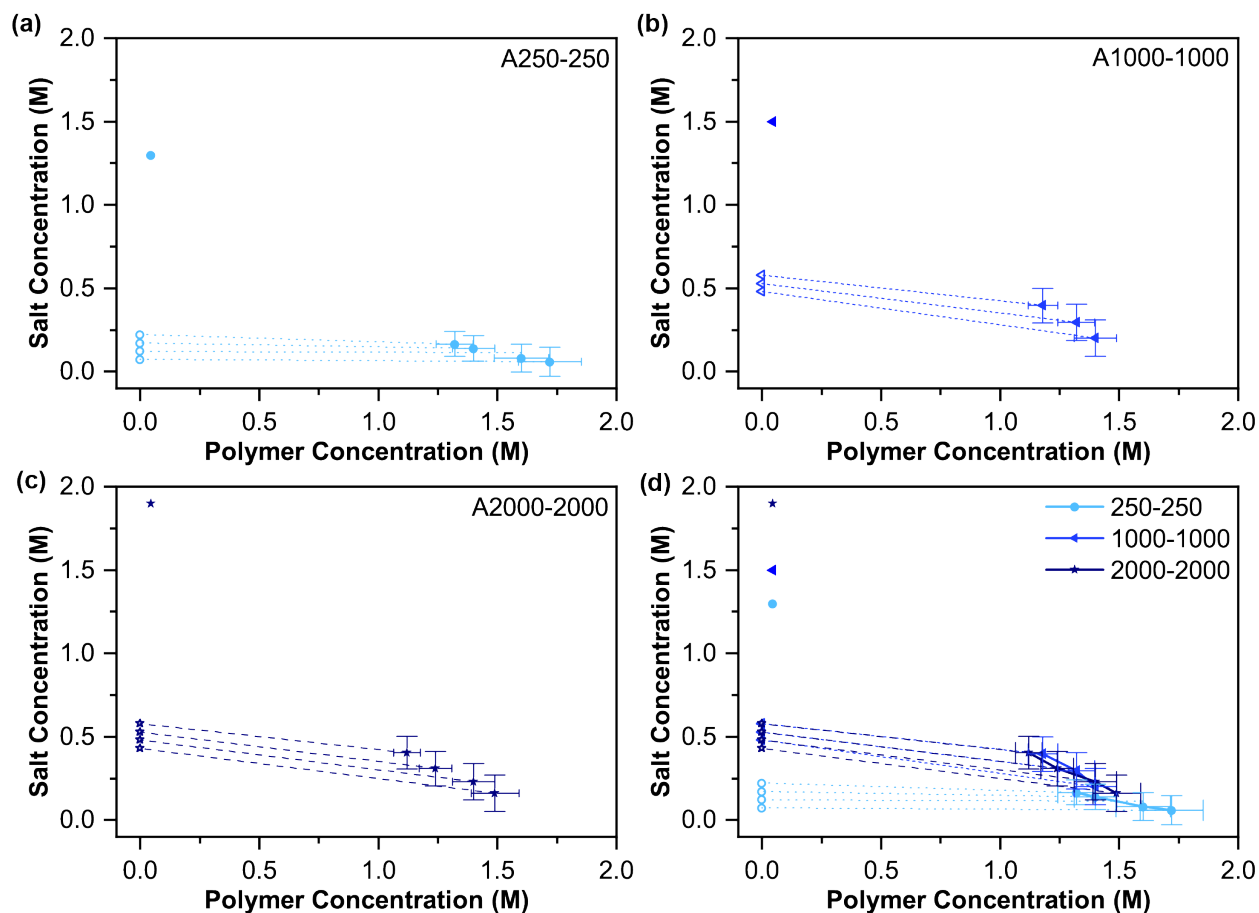


Figure S10. Experimentally determined salt-polymer phase diagrams for the complex coacervation of the acryloyl polymers PAMPS and PTMAEA in the presence of KBr at a 1:1 stoichiometric charge ratio. We compare the data for length-matched polymers with a degree of polymerization $N_{\text{anion}}-N_{\text{cation}}$ of (a) 250-250, (b) 1000-1000, (c) 2000-2000, and (d) an overlay of all three data sets. Tie lines connect data for corresponding coacervate (closed symbols) and supernatant (open symbols) sample. The unconnected symbols present at low polymer concentration and high salt concentration correspond to data obtained via turbidity analysis. Error bars in are based on the uncertainty of measurement and propagation of error.

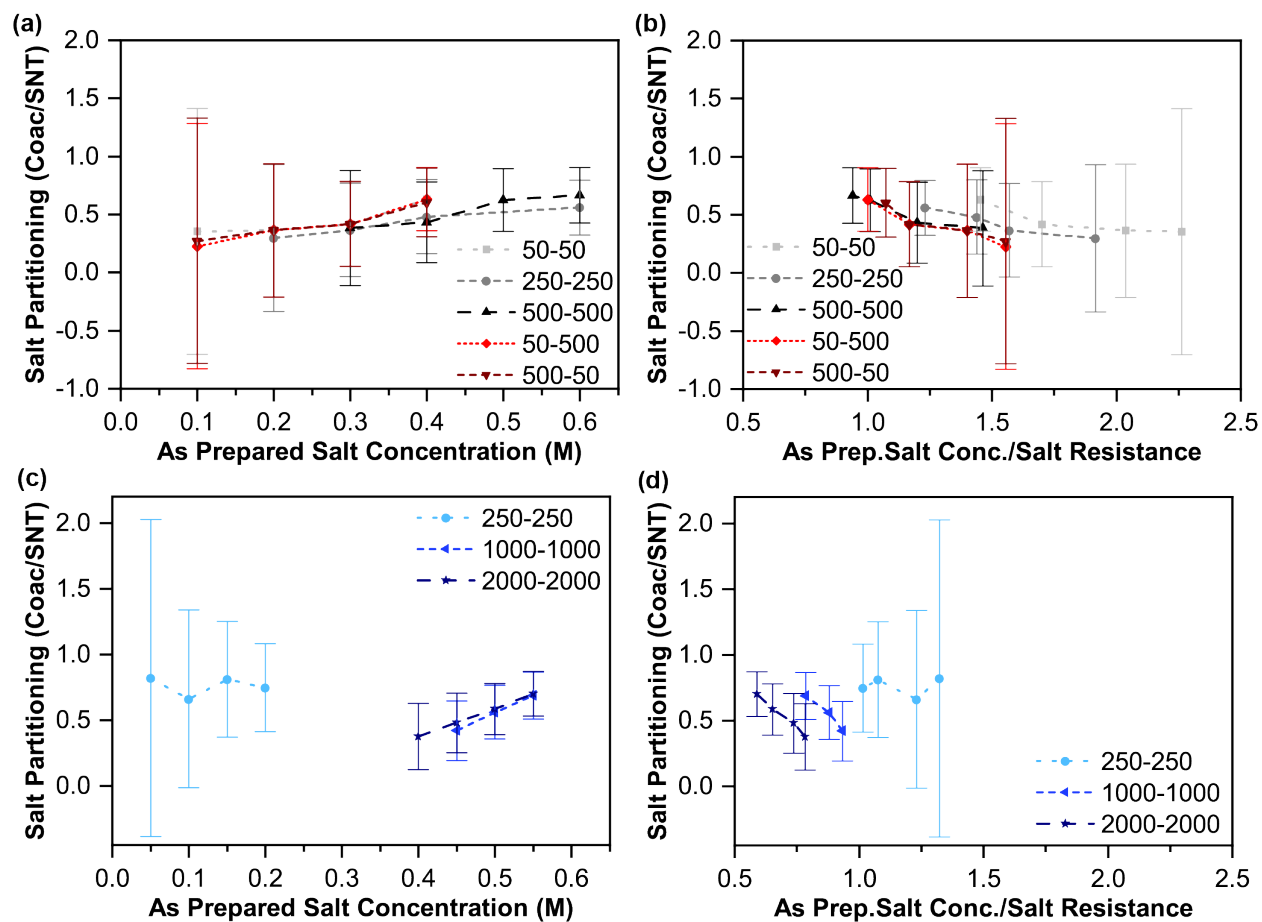


Figure S11. Salt partitioning, defined as the concentration of salt in the coacervate divided by the concentration of salt in the supernatant, as a function of the as-prepared salt concentration and the salt concentration normalized by the salt resistance at 0.045 M polymer for **(a,b)** methacryloyl polymers and **(c,d)** acryloyl polymers, respectively. Error bars are based on the uncertainty of measurement and propagation of error.

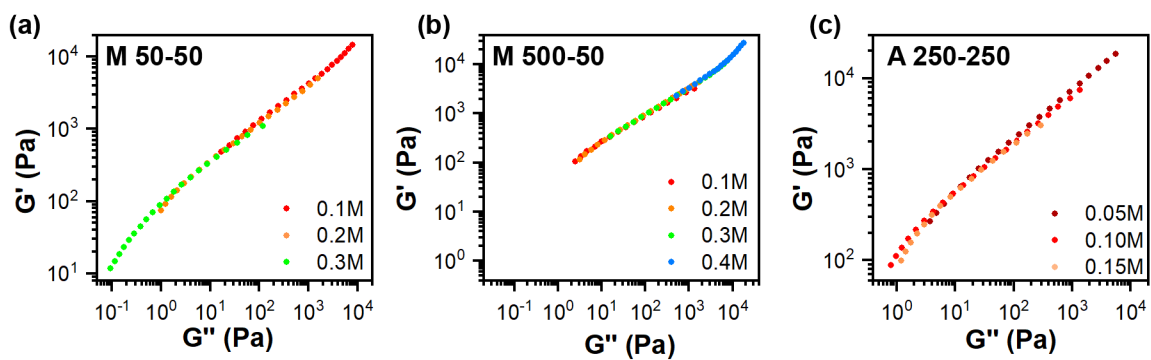


Figure S12. Selected Cole-Cole plots of G' vs. G'' , showing the continuity of the time-salt superposition, for the methacryloyl polymers with **(a)** $N \sim 50-50$ and **(b)** $N \sim 500-50$, as well as the **(c)** acryloyl polymers with $N \sim 250-250$. These samples were chosen because they displayed the largest potential deviations in the superposition (*i.e.*, samples with the shortest polymer chains, and at the highest salt concentrations).

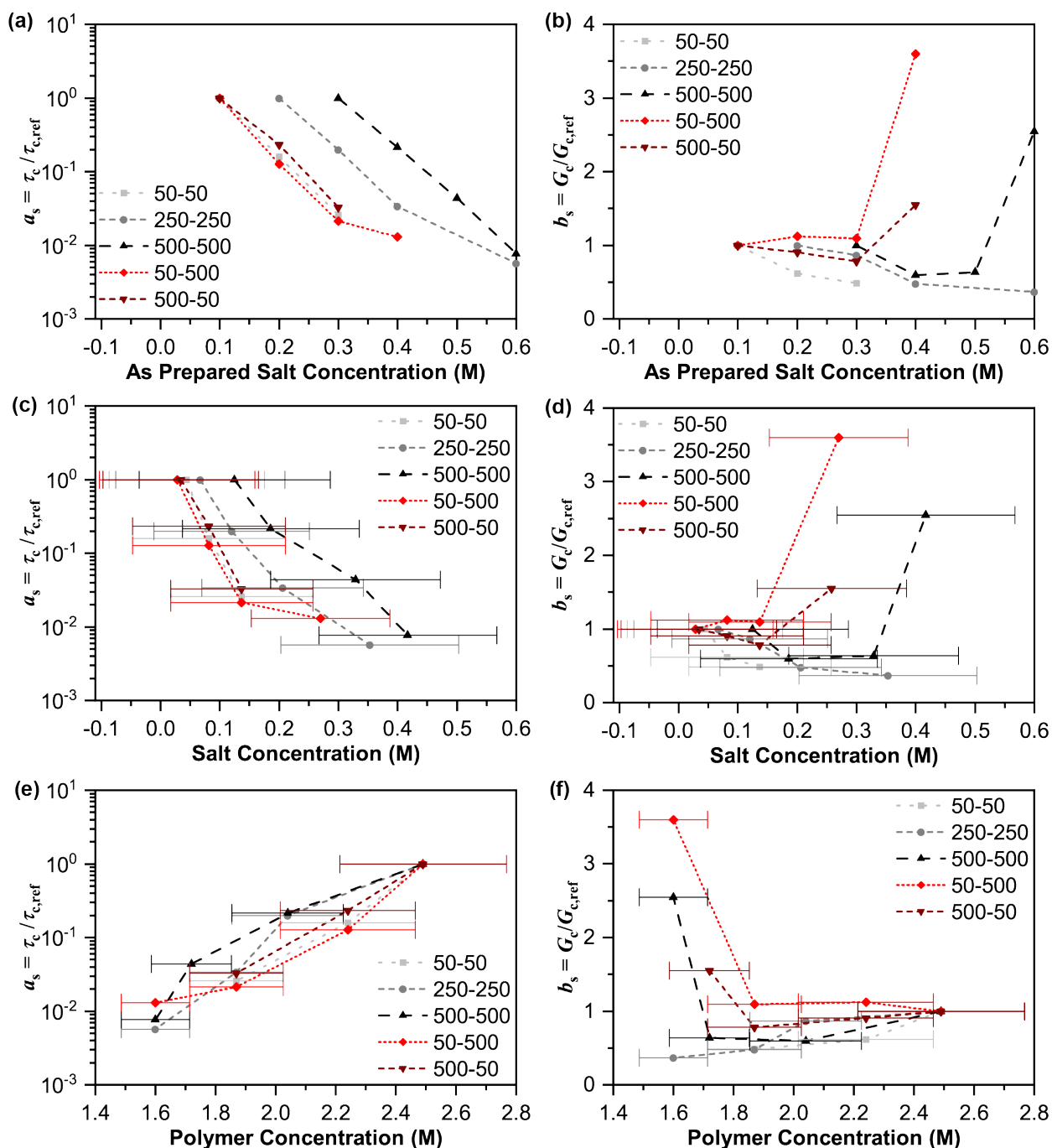


Figure S13. Graphs of the horizontal shift factor a_s and vertical shift factor b_s for cocervates formed from methacryloyl polymers with respect to **(a,b)** the as prepared salt concentration, **(c,d)** the salt concentration in the cocervate, and **(e,f)** the polymer concentration in the cocervate, respectively. Error bars come from the shift of all single curve replicates and are smaller than the symbols shown. Lines are a guide for the eye. Error bars in **(c-f)** are based on the uncertainty of measurement and propagation of error.

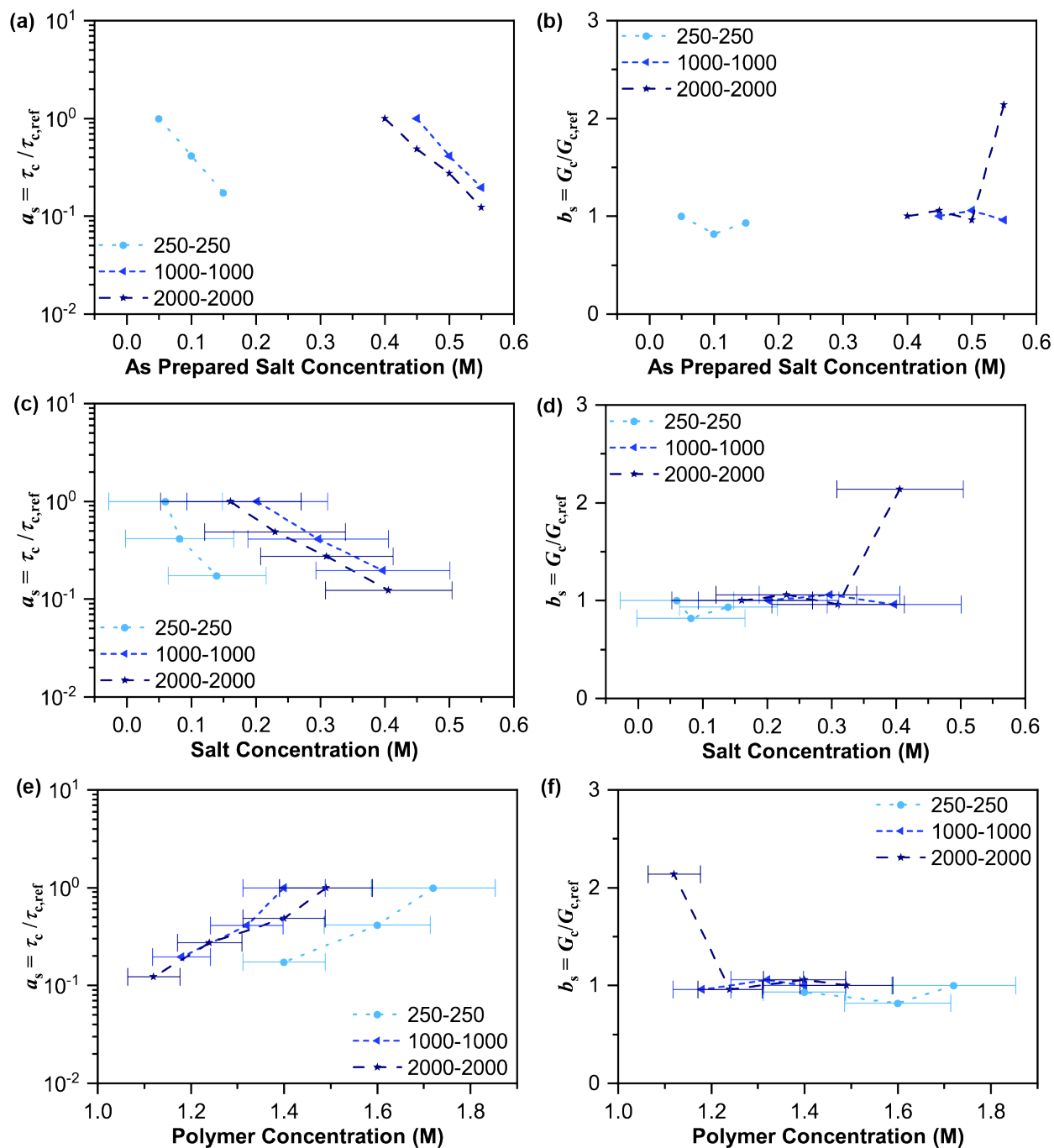


Figure S14. Graphs of the horizontal shift factor a_s and vertical shift factor b_s for coacervates formed from acryloyl polymers with respect to **(a,b)** the as prepared salt concentration, **(c,d)** the salt concentration in the coacervate, and **(e,f)** the polymer concentration in the coacervate, respectively. Error bars come from the shift of all single curve replicates and are smaller than the symbols shown. Lines are a guide for the eye. Error bars in **(c-f)** are based on the uncertainty of measurement and propagation of error.

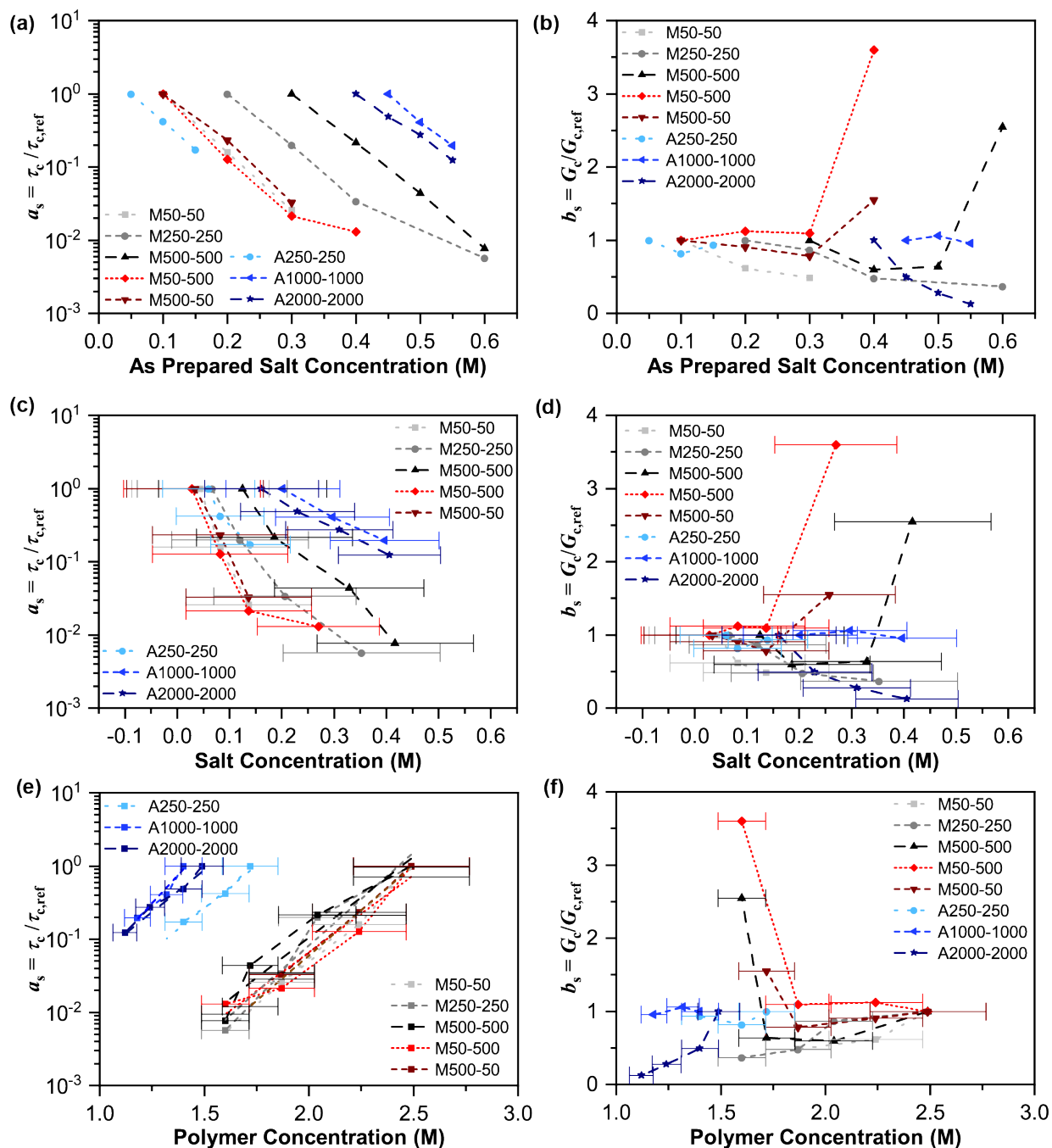


Figure S15. Graphs of the horizontal shift factor a_s and vertical shift factor b_s for coacervates formed from methacryloyl and acryloyl polymers with respect to **(a,b)** the as prepared salt concentration, **(c,d)** the salt concentration in the coacervate, and **(e,f)** the polymer concentration in the coacervate, respectively. Error bars come from the shift of all single curve replicates and are smaller than the symbols shown. Lines are a guide for the eye, except in **(e)**, where they represent an exponential fit to the data. Error bars in **(c-f)** are based on the uncertainty of measurement and propagation of error.

Table S6. Fitting parameters for horizontal shift factors a_s and salt concentration C_{salt} are fit to $\ln(a_s) = B - A\sqrt{C_{salt}}$ as in **Figure 10a-c**.

Sample	A	B	R ²
M 50-50	22.58	4.69	0.999
M 250-250	15.36	3.81	0.993
M 500-500	15.60	5.43	0.979
M 50-500	12.62	1.69	0.893
M 500-50	14.12	2.44	0.956
A 250-250	13.14	3.09	0.958
A 1000-1000	9.04	4.05	0.999
A 2000-2000	8.74	3.51	0.997

Table S7. Fitting parameters for horizontal shift factors a_s and polymer concentration $C_{polymer}$ are fit to $\ln(a_s) = AC_{polymer} - B$ as in **Figure 10d and S15e**.

Sample	A	B	R ²
M 50-50	5.80	14.58	0.986
M 250-250	5.83	14.20	0.953
M 500-500	5.09	12.37	0.927
M 50-500	4.85	12.50	0.941
M 500-50	5.67	14.12	0.998
A 250-250	5.33	9.27	0.982
A 1000-1000	7.16	10.14	0.960
A 2000-2000	5.32	8.02	0.984

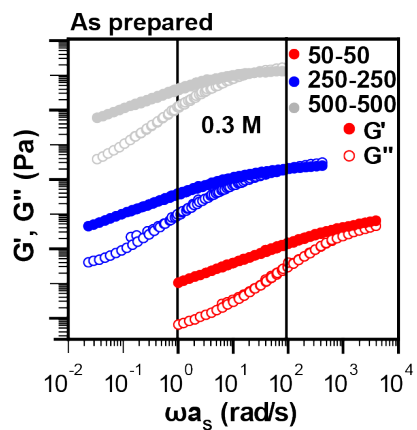


Figure S16. Plot of the time-salt superposition master curves for coacervates formed from length-matched methacryloyl polymers as a function of frequency. The data between the two vertical lines are the frequency sweep data that was collected directly at the as prepared salt concentration of 0.3 M (corresponding to a salt concentration in the coacervate of 0.137 M, 0.120 M, and 0.125 M for the $N \sim 50$, 250, and 500 systems, respectively, and a polymer concentration of 1.87 M, 2.04 M, and 2.04 M for the $N \sim 50$, 250, and 500 systems, respectively). The curves have been shifted vertically for clarity.

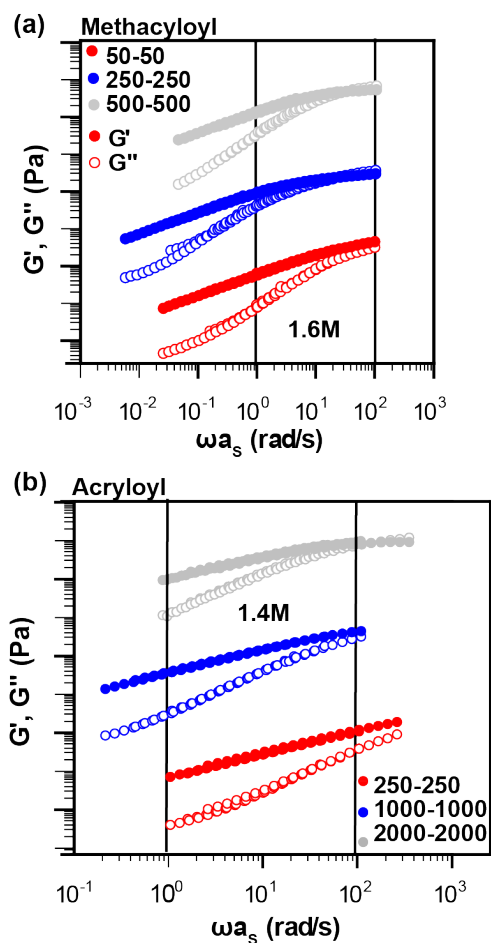


Figure S17. (a) Plot of the time-salt superposition master curves for coacervates formed from length-matched methacryloyl polymers with degree of polymerization $N \sim 50, 250,$ and 500 as a function of frequency. The data between the two vertical lines are the frequency sweep data that was collected directly at a polymer concentration in coacervate phase of 1.6 M , and were used as the reference condition. This corresponds to using the samples prepared at a KBr concentration of $0.40\text{ M}, 0.60\text{ M},$ and 0.60 M for the $N \sim 50, 250,$ and 500 systems, respectively. **(b)** Plot of the time-salt superposition master curves for coacervates formed from acryloyl polymers with degree of polymerization $N \sim 250, 1000,$ and 2000 as a function of frequency. The data between the two vertical lines are the frequency sweep data that was collected directly at a polymer concentration in coacervate phase of 1.4 M , and were used as the reference condition. This corresponds to using the samples prepared at a KBr concentration of $0.15\text{ M}, 0.45\text{ M},$ and 0.45 M for the $N \sim 250, 1000,$ and 2000 systems, respectively. Curves are shifted vertically for clarity.

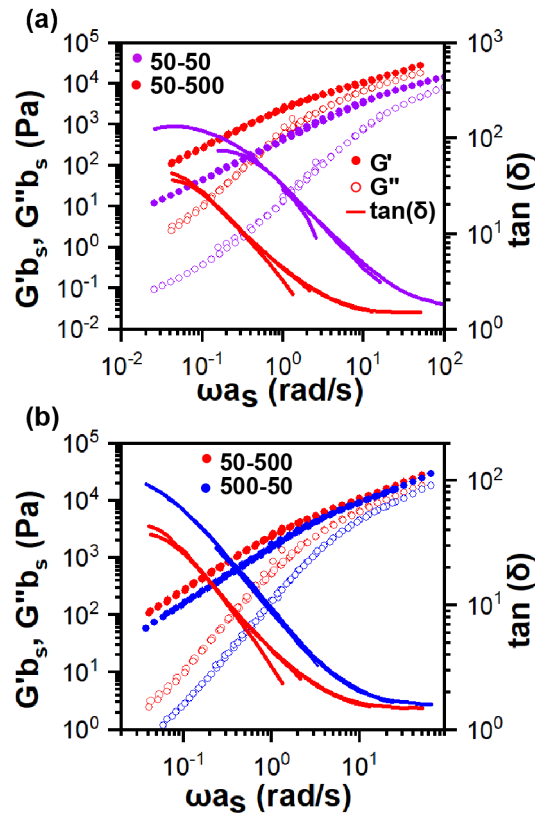


Figure S18. Graphs of the time-salt superposition master curves for coacervates formed from mismatched methacryloyl polymers with respect to frequency. **(a)** Compares the data for $N_{\text{anion}} - N_{\text{cation}}$ 500-50 with the length-matched 50-50 sample, while **(b)** compares the two mis-matched samples to each other. All datasets were shifted using the as-prepared 0.1 M KBr sample as the reference, as in **Figures 5,7**. The slight difference in the data for the two mismatched materials in **(b)** is likely due to the slightly longer degree of polymerization for the polycation present in the red curve ($N_{\text{anion}} - N_{\text{cation}} = 45-470$), as compared to the blue curve ($N_{\text{anion}} - N_{\text{cation}} = 450-47$), as reported in Table S1.